Biomech Model Mechanobiol
DOI 10.1007/s10237-013-0489-9

ORIGINAL PAPER

Modeling electrical power absorption and thermally-induced biological tissue damage

T. I. Zohdi

Received: 7 February 2013 / Accepted: 28 March 2013

Abstract This work develops a model for thermally induced damage from high current flow through biological tissue. Using the first law of thermodynamics, the balance of energy produced by the current and the energy absorbed by the tissue are investigated. The tissue damage is correlated with an evolution law that is activated upon exceeding a temperature threshold. As an example, the Fung material model is used. For certain parameter choices, the Fung material law has the ability to absorb relatively significant amounts of energy, due to its inherent exponential response character, thus, to some extent, mitigating possible tissue damage. Numerical examples are provided to illustrate the model's behavior.

Keywords Bio-tissue · Joule heating · Damage

1 Introduction

There are between one and two thousand accidental deaths per year in the Europe and United States from electrical shock, as well as countless accidents involving electrically induced tissue damage. There are a variety of detrimental effects depending on the type of affected tissue, the loading duration, and the intensity of the current and electrical fields. The primary focus of this paper is on third and fourth degree burning of tissue that arises due to the absorption of electrical energy and its conversion into heat (Joule heating). For example, with respect to layers of dermal tissue, third degree burns extend through the entire dermis, resulting in a loss of elasticity (stiffening) and tissue dryness. Fourth degree burns extend through the subcutaneous skin tissue to the muscle and bone leading to a charred, dry, stiff material. The result is that the tissue must usually be excised and limbs must be amputated, due to risk of gangrene. Fourth degree burns from electrical sources are usually fatal, primarily because they penetrate deep into the subsurface of the body. For more observations, we refer readers to Cushing (2011), Lederer and Kroesen (2005), Fontanarosa (1993), Adukauskiene et al. (2007), Cooper (1995), and Xu et al. (1999). In this paper, we will focus on electrically induced burning. Because of the complexity of associated experiments, models are needed to investigate this phenomena in a systematic manner. There has been very little analysis, from a thermo-mechanics point of view, on this topic. The objective of this paper is to utilize the first law of thermodynamics to ascertain the detrimental effects of Joule heating and subsequent temperature-induced damage, arising from high current flow through inherently resistive biological tissue.

Remark Although outside the scope of the present paper, in many cases, low intensity electrical damage does not induce significant burning of the tissue but manifests itself through organ and neurological malfunction, primarily in heart (cardiac disrhythmia) and brain tissue. For example, current as low as 30 mA at 60 Hz can case cardiac arrest, due to organ disruption, as well as secondary effects, such as respiratory failure. This is of concern due to the fact electrically based medical treatments are widespread, such as cardiac defribulation, neurological simulation, and electroconvulsive therapy for mental illness, which is a somewhat controversial practice.

2 Electrical energy absorption

The flow of current through materials usually leads to the phenomena of Joule heating (Fig. 1). The interconversions

T. I. Zohdi (✉)
Department of Mechanical Engineering,
University of California, Berkeley, CA 94720-1740, USA
e-mail: zohdi@me.berkeley.edu

Published online: 16 April 2013

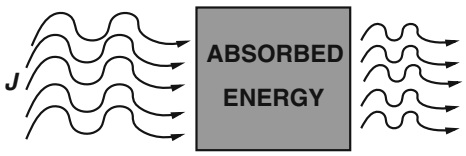

Fig. 1 Electrical flow through bio-tissue

of various forms of energy (electromagnetic, thermal, etc) in a system are governed by the first law of thermodynamics, for example, in the reference configuration

$$\rho_o \dot{w} - \boldsymbol{S} : \dot{\boldsymbol{E}} + \nabla_X \cdot \boldsymbol{q}_o - JZ = 0, \tag{2.1}$$

where ρ_o is the mass density in the reference configuration, w is the stored energy per unit mass, $\boldsymbol{S}$ is Second Piola Kirchhoff stress[1], $\boldsymbol{E}$ is the Green-Lagrange strain, $\boldsymbol{q}_o$ is heat flux in the reference configuration, J is the Jacobian of the deformation gradient, $J = det\boldsymbol{F}$ where $\boldsymbol{F} = \nabla_X \boldsymbol{x}$, $\boldsymbol{X}$ and $\boldsymbol{x}$ are the reference and current coordinates respectively. The Joule heating term $Z = a\,(\boldsymbol{\mathcal{J}} \cdot \boldsymbol{\mathcal{E}})$ is the product of the current, $\boldsymbol{\mathcal{J}}$, the electric field, $\boldsymbol{\mathcal{E}}$, and an absorption constant $0 \leq a \leq 1$. It represents the rate of electromagnetic energy absorbed due to Joule heating (a source term scaled by the Jacobian for the reference configuration). Through Ohm's law, $\boldsymbol{\mathcal{J}} = \boldsymbol{\sigma} \cdot \boldsymbol{\mathcal{E}}$, where $\boldsymbol{\sigma}$ is the material conductivity, thus $Z = a\left(\boldsymbol{\mathcal{J}} \cdot \boldsymbol{\sigma}^{-1} \cdot \boldsymbol{\mathcal{J}}\right)$. We consider the current $\boldsymbol{\mathcal{J}}$ to be given. More comments on Joule heating are provided in the "Appendix".

3 Simplifying assumptions

We adopt the following assumptions:

- We ignore thermal conduction and heat flux, hence $\nabla_X \cdot \boldsymbol{q}_o = 0$,
- All thermal and inelastic strains are negligible relative to other effects under consideration and
- Thermal damage of the tissue is characterized by a loss of tissue compliance (stiffening).

In order to isolate the effects of material changes, we consider a material point undergoing a fixed homogeneous deformation of the form $\boldsymbol{x} = \boldsymbol{G} \cdot \boldsymbol{X} \Rightarrow \boldsymbol{F} = \boldsymbol{G}$, where $\boldsymbol{G}$ is a constant second-order tensor. We consider a decomposition of the thermo-mechanical stored energy per unit mass:

$$w = C(\theta - \theta_o) + \frac{W}{\rho_o}, \tag{3.1}$$

where C is the heat capacity, θ is the temperature, θ_o is the reference temperature, and W is the elastic stored energy. Inserting this into the first law yields:

$$\rho_o C \dot{\theta} = \boldsymbol{S} : \dot{\boldsymbol{E}} - \dot{W} - \nabla_X \cdot \boldsymbol{q}_o + JZ. \tag{3.2}$$

The residual from the difference between the stress-power and the temporal derivative of W is attributed to material changes is denoted $\dot{W}^{MC}$. Explicitly, it is

$$\dot{W}^{MC} \stackrel{\text{def}}{=} \boldsymbol{S} : \dot{\boldsymbol{E}} - \dot{W}. \tag{3.3}$$

Thus, the first law of thermodynamics reads as

$$\rho_o C \dot{\theta} = \dot{W}^{MC} + JZ. \tag{3.4}$$

$\dot{W}^{MC}$ represents a power absorption term by the material as it loses compliance (materially stiffens). As an example, in order to characterize $\dot{W}^{MC}$, we consider a form of the well-known Fung material model [isotropic stiffening "soft" tissue, (Fung 1967, 1973, 1983)]:

$$W = \frac{1}{2}\boldsymbol{E} : \boldsymbol{\mathbb{H}} : \boldsymbol{E} + \mathbb{D}\left(e^{Q} - 1\right), \tag{3.5}$$

where $Q = \frac{\boldsymbol{E}:\boldsymbol{\mathbb{B}}:\boldsymbol{E}}{2}$, $\boldsymbol{\mathbb{H}}$, $\mathbb{D}$ and $\boldsymbol{\mathbb{B}}$ are material parameters and $\boldsymbol{E}$ is the Green-Lagrange strain, $\boldsymbol{E} = \frac{1}{2}\left(\boldsymbol{F}^T \cdot \boldsymbol{F} - \boldsymbol{1}\right)$. This yields:

$$\dot{W}^{MC} = -\left(\frac{1}{2}\boldsymbol{E} : \dot{\boldsymbol{\mathbb{H}}} : \boldsymbol{E} + \dot{\mathbb{D}}\left(e^{Q} - 1\right) + \frac{1}{2}\mathbb{D}e^{Q}\boldsymbol{E} : \dot{\boldsymbol{\mathbb{B}}} : \boldsymbol{E}\right). \tag{3.6}$$

Remark For the material point analysis with fixed $\boldsymbol{F}$, we note that since the material is losing compliance (becoming stiffer), then $\dot{W}^{MC} < 0$. Clearly, the role of $\dot{W}^{MC}$ is as a Joule heating energy absorber.

3.1 Material parameter choices

A finite deformation material law must match, when perturbed around the undeformed configuration, the infinitesimal deformation response, Hooke's Law, $\boldsymbol{\sigma} = \boldsymbol{\mathbb{E}} : \boldsymbol{\epsilon}$, where $\boldsymbol{\sigma}$ is the Cauchy stress, $\boldsymbol{\mathbb{E}}$ is the linear elasticity tensor, and $\boldsymbol{\epsilon}$ is the infinitesimal strain tensor.[2] In order to match the Fung material law to the linearized response at infinitesimal strains, we compute the Second Piola–Kirchhoff stress

$$\boldsymbol{S} = \frac{\partial W}{\partial \boldsymbol{E}} = \boldsymbol{\mathbb{H}} : \boldsymbol{E} + \mathbb{D}e^{Q}\frac{\partial Q}{\partial \boldsymbol{E}} = \boldsymbol{\mathbb{H}} : \boldsymbol{E} + \mathbb{D}e^{Q}\boldsymbol{\mathbb{B}} : \boldsymbol{E} \tag{3.7}$$

and

$$\begin{aligned}\boldsymbol{\mathbb{E}}^{tan} = \frac{\partial^2 W}{\partial \boldsymbol{E}^2} &= \boldsymbol{\mathbb{H}} + \mathbb{D}e^{Q}\left(\frac{\partial Q}{\partial \boldsymbol{E}} \otimes \frac{\partial Q}{\partial \boldsymbol{E}} + \frac{\partial^2 Q}{\partial \boldsymbol{E}^2}\right) \\ &= \boldsymbol{\mathbb{H}} + \mathbb{D}e^{Q}\left((\boldsymbol{\mathbb{B}} : \boldsymbol{E}) \otimes (\boldsymbol{\mathbb{B}} : \boldsymbol{E}) + \boldsymbol{\mathbb{B}}\right).\end{aligned} \tag{3.8}$$

[1] The Second Piola-Kirchhoff stress is related to the Cauchy stress ($\boldsymbol{T}$) via $\boldsymbol{T} = \frac{1}{J}\boldsymbol{F} \cdot \boldsymbol{S} \cdot \boldsymbol{F}^T$. Although we will employ referential formulations in the analysis to follow, we note that in the current configuration we have $\rho\dot{\boldsymbol{v}} - \boldsymbol{T} : \nabla_x \dot{\boldsymbol{v}} + \nabla_x \cdot \boldsymbol{q} - Z = 0$, where $\boldsymbol{T}$ is the Cauchy stress, $\boldsymbol{v}$ is the material velocity, ρ is the density, and $\boldsymbol{q}$ is the heat flux.

[2] In the case of isotropy, Hooke's law can be written in terms of the bulk κ and shear moduli μ as $\boldsymbol{\sigma} = \boldsymbol{\mathbb{E}} : \boldsymbol{\epsilon} = 3\kappa\frac{tr(\boldsymbol{\epsilon})}{3}\boldsymbol{1} + 2\mu\boldsymbol{\epsilon}'$, where $\boldsymbol{\epsilon}' = \boldsymbol{\epsilon} - \frac{tr(\boldsymbol{\epsilon})}{3}\boldsymbol{1}$.

As $\boldsymbol{E} \to \boldsymbol{0}$, we must have $\mathbb{H} + \mathbb{D}\mathbb{B} \to \mathbb{E}$, in order to match linearized response at infinitesimal strains (by matching the tangent moduli), we enforce $\mathbb{H}^o + \mathbb{D}^o\mathbb{B}^o = \mathbb{E}^o$, where the undamaged material parameters are $\mathbb{H} = \mathbb{H}^o$, $\mathbb{D} = \mathbb{D}^o$, $\mathbb{B} = \mathbb{B}^o$ and $\mathbb{E} = \mathbb{E}^o$.

Remark 1 In the analysis to follow, we make the following specific choice $\mathbb{H} = \mathbb{H}^o = \boldsymbol{0}$, thus

$$\dot{W}^{MC} = -\left(\dot{\mathbb{D}}\left(e^{Q} - 1\right) + \frac{1}{2}\mathbb{D}e^{Q}\boldsymbol{E} : \dot{\mathbb{B}} : \boldsymbol{E}\right) \tag{3.9}$$

The choice of $\mathbb{H} = \mathbb{H}^o = \boldsymbol{0}$ forces us to choose $\mathbb{D}^o\mathbb{B}^o = \mathbb{E}^o$.

Remark 2 For overviews of a wide variety of soft tissue models, see the extensive works of Holzapfel (2001), Holzapfel and Ogden (2009), or Humphrey (2002, 2003). The material constants used in the present analysis are *effective parameters*. Generally, these types of materials will contain a large number of microscale inhomogeneities. A detailed analysis of the response of the microstructure to electrical loading is beyond the scope of this paper (it is discussed in the conclusions).

Remark 3 There are a number of methods to estimate the overall effective (macroscopic) properties of materials consisting of a matrix, containing a distribution of inhomogeneities, pores, or cracks, in terms of microstructural parameters. The literature on this topic is quite extensive, dating back to the early works of Maxwell (1867, 1873) and Rayleigh (1892). For an wide-ranging overview of random heterogeneous media, see Torquato (2002) for more mathematical homogenization aspects, see Jikov et al. (1994), for solid mechanics issues, see Hashin (1983), Markov (2000), Mura (1993), Nemat-Nasser and Hori (1999), Huet (1982, 1984), for analyses of defect-laden, porous, and cracked media, see Kachanov (1993), Kachanov et al. (1994), Kachanov and Sevostianov (2005), Sevostianov et al. (2001), Sevostianov and Kachanov (2008) and for computational aspects, see Zohdi and Wriggers (2008).

4 Thermal damage and material changes

As a model problem, we consider a simple characterization of stiffening, motivated by observations associated with third and fourth degree charring/burning of tissue by electrical power absorption. We describe this classical scalar damage formulations of the form $\mathbb{E}(t) = \alpha(t)\mathbb{E}(t=0) \stackrel{\text{def}}{=} \alpha(t)\mathbb{E}^o$, where $\mathbb{E}(t)$ is the elasticity tensor and α is a scalar stiffening parameter ($1 \leq \alpha \leq \infty$) governed by[3]:

- For $\theta(t) > \theta^*$:

$$\dot{\alpha} = C_\alpha \left(\frac{\theta}{\theta^*} - 1\right), \tag{4.1}$$

- For $\theta(t) \leq \theta^*$: $\dot{\alpha} = 0$.

In the case of a structural mechanics applications, for example using a Hookean or Kirchhoff-St.Venant material, damage is usually applied in the form $\alpha\mathbb{E}^o$ (although usually with $0 \leq \alpha \leq 1$), which, in the case of isotropy, implies $\alpha\kappa^o$ and $\alpha\mu^o$, where κ^o and μ^o are the undamaged bulk and shear moduli respectively. With this type of evolution law as a motivation for the Fung material model, and in order to illustrate the mathematical model clearly, we will consider two separate stiffening damage modes, namely (I) stiffening damage occurring on $\mathbb{D}$ only and (II) stiffening damage occurring on $\mathbb{B}$ only.

4.1 Case I: $\dot{\mathbb{D}} \neq 0$ and $\dot{\mathbb{B}} = \boldsymbol{0}$

For the case of stiffening damage occurring only on $\mathbb{D}$, we have $\dot{\mathbb{B}} = \boldsymbol{0}$ ($\mathbb{B} = \mathbb{B}^o$), thus

$$\dot{W}^{MC} = -\frac{1}{2}\dot{\mathbb{D}}\left(e^{\frac{\boldsymbol{E}:\mathbb{B}^o:\boldsymbol{E}}{2}} - 1\right). \tag{4.2}$$

If we assume $\mathbb{D} = \alpha\mathbb{D}^o$, where α is governed by Eq. 4.1, we obtain

$$\dot{W}^{MC} = -\frac{1}{2}\dot{\alpha}\mathbb{D}^o\left(e^{\frac{\boldsymbol{E}:\mathbb{B}^o:\boldsymbol{E}}{2}} - 1\right). \tag{4.3}$$

4.2 Case II: $\dot{\mathbb{D}} = 0$ and $\dot{\mathbb{B}} \neq \boldsymbol{0}$

For the case of stiffening damage occurring only on $\mathbb{B}$, we have $\dot{\mathbb{D}} = 0$ ($\mathbb{D} = \mathbb{D}^o$), thus

$$\dot{W}^{MC} = -\frac{1}{2}\mathbb{D}\left(e^{\frac{\boldsymbol{E}:\mathbb{B}:\boldsymbol{E}}{2}}\boldsymbol{E} : \dot{\mathbb{B}} : \boldsymbol{E}\right). \tag{4.4}$$

If we assume $\mathbb{B} = \alpha\mathbb{B}^o$, where α is governed by Eq. 4.1, we obtain

$$\dot{W}^{MC} = -\frac{1}{2}\mathbb{D}^o\left(e^{\frac{\boldsymbol{E}:(\alpha\mathbb{B}^o):\boldsymbol{E}}{2}}\boldsymbol{E} : (\dot{\alpha}\mathbb{B}^o) : \boldsymbol{E}\right). \tag{4.5}$$

Remark Of course, there are many possible choices for parameter combinations (for example mixing the stiffening damage modes), and this would depend on the specific tissue type.

5 Temperature evolution-examples

Our material point model problem (with $\boldsymbol{F}$ fixed and no heat flux) yields the following evolution equation for the temperature

[3] For further details on these types of phenomenological (damage) formulations, the interested reader is referred to the seminal work of Kachanov (1986).

$$\dot{\theta} = \frac{1}{\rho_o C}\left(aJ\boldsymbol{\mathcal{J}}\cdot\boldsymbol{\sigma}^{-1}\cdot\boldsymbol{\mathcal{J}} + \dot{W}^{MC}\right) \stackrel{\text{def}}{=} \Lambda(\theta), \tag{5.1}$$

where we note that since the material is losing compliance (becoming stiffer), then $\dot{W}^{MC} \leq 0$. Clearly, when $\Lambda(\theta) > 0$, then the temperature will grow, and for $\Lambda(\theta) < 0$ the temperature will decrease. In theory, the last case ($\Lambda(\theta) < 0$) can occur, provided the material absorbs all of the Joule heating energy and continues to stiffen, essentially leading to an endothermic response. The governing equation is stepped forward in time with a simple explicit time-marching scheme

$$\theta(t + \Delta t) = \theta(t) + \Delta t\,\Lambda(\theta(t)). \tag{5.2}$$

The parameters used in the model were

- The thermal threshold parameter: $\theta^* = 400\,\text{K}$,
- The starting (human body) temperature: $\theta_o = 310\,\text{K}$,
- The current: $||\boldsymbol{\mathcal{J}}|| = 50,000\,\text{A}$,
- The bulk modulus: $\kappa^o = 1.0\,\text{GPa}$,
- The shear modulus: $\mu^o = 0.5\,\text{GPa}$,
- The Joule heating absorption coefficient: $a = 1$,
- The mass density: $\rho_o = 1,000\,\text{kg/m}^3$,
- The heat capacity: $C = 10^2\,\text{J/(kg}-\text{K)}$,
- The stiffening damage rate: $C_\alpha = 1$ and
- The isotropic conductivity ($\boldsymbol{\sigma} = \sigma\mathbf{1}$) : $\sigma = 100\,\text{S/m}$.

We remark that the parameters chosen are to exercise the model and are not correlated to any particular experiment. In order to determine the approximate time scales involved for this process to occur, we considered constant Joule heating, with no stiffening damage, given by

$$\dot{\theta} = \frac{aJ\boldsymbol{\mathcal{J}}\cdot\boldsymbol{\sigma}^{-1}\cdot\boldsymbol{\mathcal{J}}}{\rho_o C}, \tag{5.3}$$

to attain a critical temperature, θ^*

$$\theta^* = \theta(t^*) = \underbrace{\theta(t=0)}_{\stackrel{\text{def}}{=}\theta_o} + \frac{(t^* - t_o)||\boldsymbol{\mathcal{J}}||^2}{\rho_o C\sigma}, \tag{5.4}$$

yielding (with $t_o = 0$)

$$t^* = \frac{(\theta^* - \theta_o)\rho_o C\sigma}{||\boldsymbol{\mathcal{J}}||^2}. \tag{5.5}$$

With the chosen material parameters, $t^* \approx 1.6$ seconds. We ran the simulations to approximately $5 \times t^* = 8$ seconds, in order to observe the full response of the model. Of course, temperatures of the levels computed for this longer time scale would bring in other effects, such as tissue ablation, which is currently not in the model. The plots in Figs. 2, 3 and 4 illustrate the temperature and stiffening evolution versus time for various fixed deformations, characterized by the following load (displacement) parameters:

- Figure 2: $\boldsymbol{u} = 0.1 \times \mathbf{1}\cdot\boldsymbol{X} \Rightarrow \boldsymbol{F} = 1.1 \times \mathbf{1}$,
- Figure 3: $\boldsymbol{u} = 0.5 \times \mathbf{1}\cdot\boldsymbol{X} \Rightarrow \boldsymbol{F} = 1.5 \times \mathbf{1}$ and
- Figure 4: $\boldsymbol{u} = 1.0 \times \mathbf{1}\cdot\boldsymbol{X} \Rightarrow \boldsymbol{F} = 2.0 \times \mathbf{1}$.

For Case II, the Fung law has the ability to absorb much more electrical energy, relative to Case I, due to the increase (due to α) in exponential behavior inherent in the Case II formulation, characterized by the term $e^{\frac{\boldsymbol{E}:(\alpha\boldsymbol{B}^o):\boldsymbol{E}}{2}}$ in Eq. 4.5. In the most extreme loading case, $\boldsymbol{u} = \mathbf{1}\cdot\boldsymbol{X}$, the temperature eventually decreases, since $\Lambda(\theta)$ eventually becomes negative (as α increases mildly), which is consistent with the comments made at the beginning of this section.

6 Summary and extensions

This note provided a straightforward description of electrically induced thermal tissue damage. Relatively simple numerical examples were provided to give qualitative information. However, to truly probe beyond the somewhat qualitative material point analysis presented here, for example, resolving the generation of fine-scale thermal gradients, transient electromagnetic fields, stress fields, and chemical/damage fields, one must numerically solve the coupled system of PDE's associated with (1) Maxwell's equations, (2) the first law of thermodynamics, (3) the balance of linear momentum, and (4) reaction–diffusion laws.[4] To accurately capture the coupled (transient) electromagnetic, thermal, mechanical, and chemical behavior of complex micro-electronic materials, Zohdi (2010) addressed the modeling and simulation of such strongly coupled systems using a staggered temporally adaptive FDTD (Finite Difference Time Domain) method, which is ideal for solving time-transient Maxwell's Equations. The mentioned staggered temporally adaptive FDTD framework provided a straightforward modular approach to resolving thermal effects, arising from Joule heating, which alter the pointwise material properties employing a staggered, temporally adaptive scheme. The general methodology is as follows (at a given time increment): (1) each field equation is solved individually, "freezing" the other (coupled) fields in the system, allowing only the primary field to be active, and (2) after the solution of each field equation, the primary field variable is updated, and the next field equation is treated in a similar manner. As the physics changes, the field that is most sensitive (exhibits the largest amount of relative nondimensional change) dictates the time-step size. For more details, see Zohdi (2010). We remark that while the most widely used technique is the FDTD, there are other methods, such as (a) *the Multi Resolution Time Domain Method*, which is based on

[4] For an in depth mathematical analysis of coupled thermal, diffusive and chemical effects in solids, in particular instabilities, we refer the reader to Markenscoff (2001a,b, 2003).

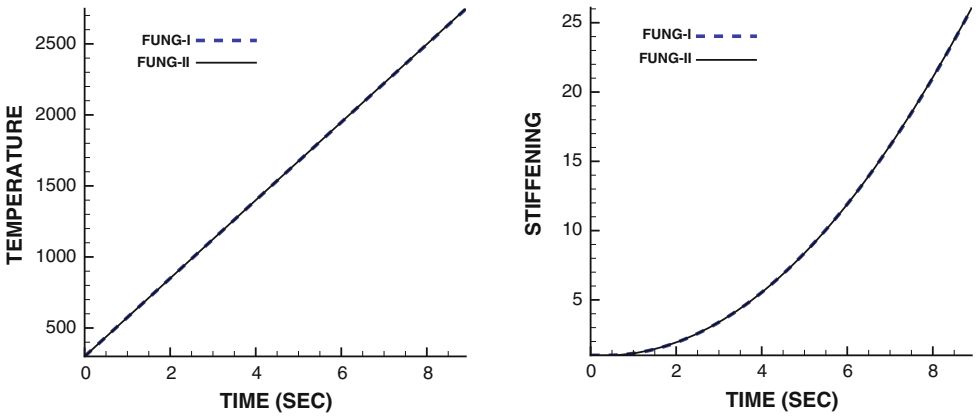

Fig. 2 Temperature evolution for Case I and Case II Fung material laws. *Left*: temperature and *Right*: stiffening (damage) parameter, α. The load (displacement) parameter used: $\boldsymbol{u} = 0.1 \times \mathbf{1} \cdot \boldsymbol{X} \Rightarrow \boldsymbol{F} = 1.1 \times \mathbf{1}$

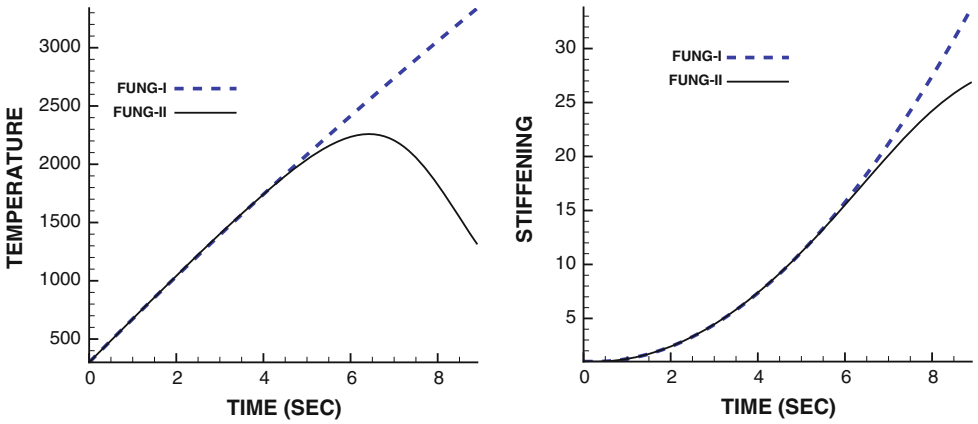

Fig. 3 Temperature evolution for Case I and Case II Fung material laws. *Left*: temperature and *Right*: stiffening (damage) parameter, α. The load (displacement) parameter used: $\boldsymbol{u} = 0.5 \times \mathbf{1} \cdot \boldsymbol{X} \Rightarrow \boldsymbol{F} = 1.5 \times \mathbf{1}$

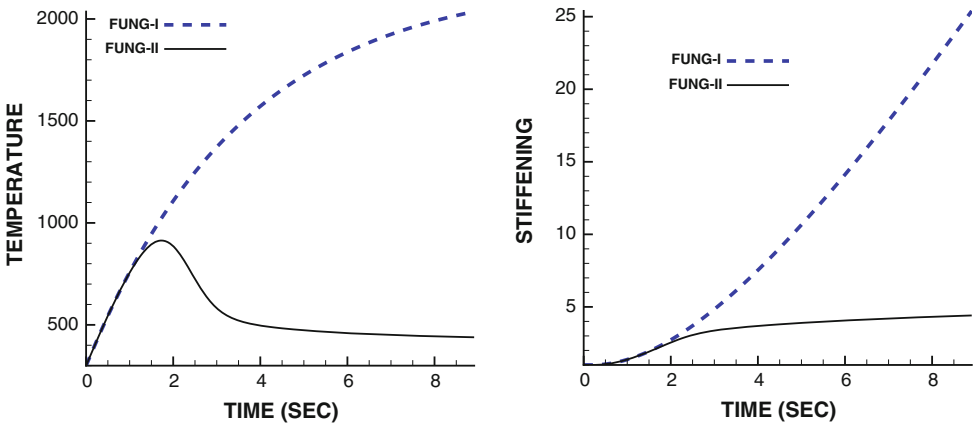

Fig. 4 Temperature evolution for Case I and Case II Fung material laws. *Left*: temperature and *Right*: stiffening (damage) parameter, α. The load (displacement) parameter used: $\boldsymbol{u} = \mathbf{1} \cdot \boldsymbol{X} \Rightarrow \boldsymbol{F} = 2 \times \mathbf{1}$

wavelet-based discretization, (b) *the Finite Element Method*, which is based on discretization of variational formulations and which are ideal for irregular geometries (see Demkowicz (2006); Demkowicz et al. (2007) for the state of the art in adaptive Finite Element Methods for Maxwell's equations), (c) *the Pseudo Spectral Time Domain Method*, which is based on Fourier and Chebyshev transforms, followed by a lattice or grid discretization of the transformed domain, (d) *the Discrete Dipole Approximation*, which is based on an array of dipoles solved iteratively with the Conjugate Gradient method and a Fast Fourier Transform to multiply matrices, (e) *the Method of Moments*, which is based on integral formu-

lations employing Boundary Element Method discretization, often accompanied by the Fast Multipole Method to accelerate summations needed during the calculations, and (f) *the Partial Element Equivalent Circuit Method*, which is based on integral equations that are interpreted as circuits in discretization cells. We remark that extensions to damage that occurs in induced electromechanics tissue, in particular that of the heart, is one possible avenue to apply this type of analysis. For recent work in this area, see the works of Kuhl and co-workers (Hurtado and Kuhl 2012; Chen et al. 2011; Dal et al. 2012, 2013; Wong et al. 2011; Kotikanyadanam et al. 2010; Göktepe and Kuhl 2010). The development of numerical methods for electrically induced tissue damage, drawing upon FDTD and harnessing features of methods (a)–(f), is under further investigation by the author. These more detailed techniques may also shed light on low intensity electrical damage, which can lead to organ and neurological malfunction.

7 Appendix: Joule heating

Joule heating can be explicitly identified by considering Faraday's Law

$$\nabla \times \boldsymbol{\mathcal{E}} = -\frac{\partial \boldsymbol{\mathcal{B}}}{\partial t} \tag{7.1}$$

and Ampere's Law

$$\nabla \times \boldsymbol{\mathcal{H}} = \frac{\partial \boldsymbol{\mathcal{D}}}{\partial t} + \boldsymbol{\mathcal{J}} \tag{7.2}$$

where we recall that $\boldsymbol{\mathcal{E}}$ is the electric field, $\boldsymbol{\mathcal{D}}$ is the electric field flux, $\boldsymbol{\mathcal{J}}$ is the electric current, $\boldsymbol{\mathcal{H}}$ is the magnetic field, and $\boldsymbol{\mathcal{B}}$ is the magnetic field flux. Joule heating can be motivated by forming the inner product of the magnetic field with Faraday's law and the inner product of the electric field with Ampere's law and forming the difference to yield

$$\underbrace{\boldsymbol{\mathcal{E}} \cdot (\nabla \times \boldsymbol{\mathcal{H}}) - \boldsymbol{\mathcal{H}} \cdot (\nabla \times \boldsymbol{\mathcal{E}})}_{-\nabla \cdot (\boldsymbol{\mathcal{E}} \times \boldsymbol{\mathcal{H}}) = -\nabla \cdot \boldsymbol{\mathcal{S}}} = \boldsymbol{\mathcal{E}} \cdot \boldsymbol{\mathcal{J}} + \underbrace{\boldsymbol{\mathcal{E}} \cdot \frac{\partial \boldsymbol{\mathcal{D}}}{\partial t} + \boldsymbol{\mathcal{H}} \cdot \frac{\partial \boldsymbol{\mathcal{B}}}{\partial t}}_{= \frac{\partial \mathcal{W}}{\partial t}}, \tag{7.3}$$

where $\mathcal{W} = \frac{1}{2}(\boldsymbol{\mathcal{E}} \cdot \boldsymbol{\mathcal{D}} + \boldsymbol{\mathcal{H}} \cdot \boldsymbol{\mathcal{B}})$ is the electromagnetic energy and where $\boldsymbol{\mathcal{S}} = \boldsymbol{\mathcal{E}} \times \boldsymbol{\mathcal{H}}$ is the Poynting vector. Thus,

$$\frac{\partial \mathcal{W}}{\partial t} + \nabla \cdot \boldsymbol{\mathcal{S}} = -\boldsymbol{\mathcal{J}} \cdot \boldsymbol{\mathcal{E}} \tag{7.4}$$

Equation 7.4 is usually referred to as Poynting's theorem and can be interpreted as stating that the rate of change of electromagnetic energy within a volume, plus the energy flowing out through the material, is equal to the negative of the total work done by the fields on the sources and electrical conduction. We consider the absorbed energy that is available for heating to be proportional to the energy associated with current flow ($\boldsymbol{\mathcal{J}} \cdot \boldsymbol{\mathcal{E}}$) in Eq. 7.4.

References

Adukauskiene D, Vizgirdaite V, Mazeikiene S (2007) Electrical injuries. Medicina (Kaunas) 43(3):259–266

Chen MQ, Wong J, Kuhl E, Giovangrandi L, Kovacs GTA (2011) Characterization of electrophysiological conduction in cardiomyocyte co-cultures using co-occurrence analysis. Comp Meth Biomech Biomed Eng. doi:10.1080/10255842.2011.615310

Cooper MA (1995) Emergent care of lightning and electrical injuries. Semin Neurol 15(3):268–78

Cushing T (2011) Electrical injuries in emergency medicine. Medscape Reference. Web. 29, September 2011

Dal H, Göktepe S, Kaliske M, Kuhl E (2012) A fully implicit finite element method for bidomain models of cardiac electrophysiology. Comp Meth Biomech Biomed Eng 15:645–656

Dal H, Göktepe S, Kaliske M, Kuhl E (2013) A fully implicit finite element method for bidomain models of cardiac electromechanics. Comp Meth Appl Mech Eng 253:323–336

Demkowicz (2006) Computing with hp-adaptive finite elements. I. One- and two- dimensional elliptic and Maxwell problems. CRC Press, Taylor and Francis

Demkowicz L, Kurtz J, Pardo D, Paszynski M, Rachowicz W, Zdunek A (2007) Computing with hp-adaptive finite elements, vol 2: frontiers: three dimensional elliptic and Maxwell problems with applications. CRC Press, Taylor and Francis

Fontanarosa PB (1993) Electrical shock and lightning strike. Ann Emerg Med 22(2 Pt 2):378–87

Fung YC (1967) Elasticity of soft tissues in simple elongation. Am J Physiol 28:1532–1544

Fung YC (1973) Biorheology of soft tissues. Biorheology 10:139–155

Fung YC (1983) On the foundations of biomechanics. ASME J Appl Mech 50:1003–1009

Göktepe S, Kuhl E (2010) Electromechanics of the heart: a unified approach to the strongly coupled excitation–contraction problem. Comp Mech 45:227–243

Hashin Z (1983) Analysis of composite materials: a survey. ASME J Appl Mech 50:481–505

Holzapfel GA (2001) Biomechanics of soft tissue. In: Lemaitre J (ed) The handbook of materials behavior models, vol III, Multiphysics behaviors, Chapter 10, Composite media, Biomaterials. Academic Press, Boston, pp 1049–1063

Holzapfel GA, Ogden RW (2009) Biomechanical modeling at the molecular, cellular and tissue levels. Springer, Berlin

Huet C (1982) Universal conditions for assimilation of a heterogeneous material to an effective medium. Mech Res Commun 9(3):165–170

Huet C (1984) On the definition and experimental determination of effective constitutive equations for heterogeneous materials. Mech Res Commun 11(3):195–200

Humphrey JD (2002) Cardiovascular solid mechanics. Cells, tissues, and organs. Springer, New York

Humphrey JD (2003) Continuum biomechanics of soft biological tissues. Proc R Soc 459(2029):3–46

Hurtado D, Kuhl E (2012) Computational modeling of electrocardiograms: Repolarization and T-wave polarity in the human heart. Comp Meth Biomech Biomed Eng. doi:10.1080/10255842.2012.729582

Jikov VV, Kozlov SM, Olenik OA (1994) Homogenization of differential operators and integral functionals. Springer, Berlin

Kachanov LM (1986) Introduction to continuum damage mechanics. Martinus Nijoff, Dordricht

Kachanov M (1993) Elastic solids with many cracks and related problems. Advance applied mechanics, vol 30. Academic Press, New York

Kachanov M, Tsukrov I, Shafiro B (1994) Effective moduli of solids with cavities of various shapes. Appl Mech Rev 47:S151–S174

Kachanov M, Sevostianov I (2005) On the quantitative characterization of microstructures and effective properties. Int J Solids Struct 42:309–336

Kotikanyadanam M, Göktepe S, Kuhl E (2010) Computational modeling of electrocardiograms: a finite element approach towards cardiac excitation. Int J Num Meth Biomed Eng 26:524–533

Lederer W, Kroesen G (2005) Emergency treatment of injuries following lightning and electrical accidents. Anaesthesist 54(11):1120–9

Markenscoff X (2001a) Diffusion induced instability. Q Appl Mech LIX(1):147–151

Markenscoff X (2001b) Instabilities of a thermo-mechano-chemical system. Q Appl Mech LIX(3):471–477

Markenscoff X (2003) On conditions of "negative creep" in amorphous solids. Mech Mater 35(3–6):553–557

Markov KZ (2000) Elementary micromechanics of heterogeneous media. In: Markov KZ, Preziozi L (eds) Heterogeneous media: micromechanics modeling methods and simulations. Birkhauser, Boston, pp 1–162

Maxwell JC (1867) On the dynamical theory of gases. Philos Trans Soc Lond. 157:49

Maxwell JC (1873) A treatise on electricity and magnetism, 3rd edn. Clarendon Press, Oxford

Mura T (1993) Micromechanics of defects in solids, 2nd edn. Kluwer, Berlin

Nemat-Nasser S, Hori M (1999) Micromechanics: overall properties of heterogeneous solids, 2nd edn. Elsevier, Amsterdam

Rayleigh JW (1892) On the influence of obstacles arranged in rectangular order upon properties of a medium. Philos Mag 32:481–491

Sevostianov I, Gorbatikh L, Kachanov M (2001) Recovery of information of porous/microcracked materials from the effective elastic/conductive properties. Mater Sci Eng A 318:1–14

Sevostianov I, Kachanov M (2008) Connections between elastic and conductive properties of heterogeneous materials. Adv Appl Mech 42:69–253

Torquato S (2002) Random heterogeneous materials: microstructure and macroscopic properties. Springer, New York

Wong J, Göktepe S, Kuhl E (2011) Computational modeling of electrochemical coupling: a novel finite element approach towards ionic models for cardiac electrophysiology. Comp Meth Appl Mech Eng 200:3139–3158

Xu X, Zhu W, Wu Y (1999) Experience of the treatment of severe electric burns on special parts of the body. Ann NY Acad Sci 888:121–130

Zohdi TI, Wriggers P (2008) Introduction to computational micromechanics. Springer, Berlin

Zohdi TI (2010) Simulation of coupled microscale multiphysical-fields in particulate-doped dielectrics with staggered adaptive FDTD. Comput Methods Appl Mech Eng 199:79–101